

## Brain imaging signatures of the relationship between epidermal nerve fibers and heat pain perception



Ming-Tsung Tseng<sup>a,\*</sup>, Yazhuo Kong<sup>b</sup>, Ming-Chang Chiang<sup>c</sup>, Chi-Chao Chao<sup>d</sup>,  
Wen-Yih I. Tseng<sup>e</sup>, Sung-Tsang Hsieh<sup>a,d,f,\*\*</sup>

<sup>a</sup> Graduate Institute of Brain and Mind Sciences, National Taiwan University College of Medicine, Taipei, Taiwan

<sup>b</sup> Oxford Center for Functional Magnetic Resonance Imaging of the Brain and Nuffield Division of Anaesthetics, Nuffield Department of Clinical Neurosciences, University of Oxford, Oxford, United Kingdom

<sup>c</sup> Department of Biomedical Engineering, National Yang-Ming University, Taipei, Taiwan

<sup>d</sup> Department of Neurology, National Taiwan University Hospital, Taipei, Taiwan

<sup>e</sup> Center for Optoelectronic Biomedicine, National Taiwan University Hospital, Taipei, Taiwan

<sup>f</sup> Department of Anatomy and Cell Biology, National Taiwan University Hospital, Taipei, Taiwan

### ARTICLE INFO

#### Article history:

Received 21 April 2015

Accepted 6 August 2015

Available online 13 August 2015

#### Keywords:

Contact heat-evoked potential  
Functional magnetic resonance imaging (fMRI)  
Psychophysical interaction analysis  
Skin innervation  
Pain  
Heat

### ABSTRACT

Although the small-diameter primary afferent fibers in the skin promptly respond to nociceptive stimuli and convey sensory inputs to the central nervous system, the neural signatures that underpin the relationship between cutaneous afferent fibers and pain perception remain elusive. We combined skin biopsy at the lateral aspect of the distal leg, which is used to quantify cutaneous afferent fibers, with fMRI, which is used to assess brain responses and functional connectivity, to investigate the relationship between cutaneous sensory nerves and the corresponding pain perception in the brain after applying heat pain stimulation to the dorsum of the right foot in healthy subjects. During painful stimulation, the degree of cutaneous innervation, as measured by epidermal nerve fiber density, was correlated with individual blood oxygen level-dependent (BOLD) signals of the posterior insular cortex and of the thalamus, periaqueductal gray, and rostral ventromedial medulla. Pain perception was associated with the activation of the anterior insular cortex and with the functional connectivity from the anterior insular cortex to the primary somatosensory cortex during painful stimulation. Most importantly, both epidermal nerve fiber density and activity in the posterior insular cortex showed a positive correlation with the strength of coupling under pain between the anterior insular cortex and the primary somatosensory cortex. Thus, our findings support the notion that the neural circuitry subserving pain perception interacts with the cerebral correlates of peripheral nociceptive fibers, which implicates an indirect role for skin nerves in human pain perception.

© 2015 Elsevier Inc. All rights reserved.

### Introduction

Sensory nerves, which belong to the small-diameter category in the most superficial layer of the skin, the epidermis, respond to nociceptive stimuli (i.e., actual or potential tissue-damaging stimuli encoded by nociceptors) and serve the sensation of pain (i.e., an unpleasant sensory and emotional experience) (Merksey and Bogduk, 1994) by transmitting these sensory inputs to the brain (Ringkamp et al., 2013; Todd and Koerber, 2013). Despite extensive studies on their functions, the data obtained from both healthy controls (Selim et al., 2010) and

neuropathic conditions (Herrmann et al., 2004; Zhou et al., 2007) have not revealed a direct correlation between skin innervation and the perception of pain, thus suggesting additional central modulations during the transmission from the periphery to the brain. In primates, anatomical tracer studies have shown that the peripheral nociceptive inputs that are received by epidermal nerves are relayed to the brainstem homeostatic centers, ascend to the thalamus, and project heavily to the posterior insular cortex (IC), primary somatosensory cortex (SI), and anterior cingulate cortex (ACC) (Craig, 2003; Dum et al., 2009; Willis et al., 2001). Although these brain regions serve as the cerebral destination of nociceptive transmission, direct evidence from functional brain imaging studies in humans is lacking concerning the central representation of skin nerves and their role in pain perception.

In contrast to the posterior IC which receives nociceptive information, the anterior IC, which has the highest incidence of activation to acute experimental pain (Apkarian et al., 2005) and displays neural activity correlated with pain perception (Coghill et al., 1999; Tseng et al., 2013b), is a region that is critical to integrating pain information with

\* Correspondence to: M.-T. Tseng, Graduate Institute of Brain and Mind Sciences, National Taiwan University College of Medicine, 1 Jen-Ai Road Section 1, Taipei 10051, Taiwan. Tel.: +886 2 23123456x88870; fax: +886 2 23224814.

\*\* Correspondence to: S.-T. Hsieh, Department of Neurology, National Taiwan University Hospital, 7 Chung-Shan South Road, Taipei 10002, Taiwan. Tel.: +886 2 23123456x8182; fax: +886 2 23915292.

E-mail addresses: [mingtsungtseng@ntu.edu.tw](mailto:mingtsungtseng@ntu.edu.tw) (M.-T. Tseng), [shsieh@ntu.edu.tw](mailto:shsieh@ntu.edu.tw) (S.-T. Hsieh).

emotional and cognitive processes to create the subjective pain experience (Baliki et al., 2009; Craig, 2009). Recent evidence indicates that the processing of pain engages the functional linkage between the anterior IC and pain-related brain areas, such as the somatosensory cortices and cingulate (Peltz et al., 2011; Wiech et al., 2010). Considering intensity to be the most salient characteristic of pain (Turk and Melzack, 1992), it is thus plausible that the functional connectivity of the anterior IC also modulates the perception of intensity in the context of pain. Moreover, because evidence suggests that the insula plays a pivotal role in transforming nociceptive inputs into pain perception (Baliki et al., 2009), it is likely that anterior IC-associated functional circuitry interacts with the posterior IC to integrate pain information that is conveyed via cutaneous afferent fibers. Nevertheless, evidence in support of these hypotheses is still missing in humans. It remains an open question whether the neural representation of pain perception is related to the neural substrates of peripheral afferent nerves.

Several groups, including ours, have developed sensitive staining techniques to visualize and quantify these cutaneous nerve terminals (Lauria et al., 2010). Recently, we demonstrated altered cerebral activity (Tseng et al., 2013a) and functional connectivity (Hsieh et al., 2015) following cutaneous nerve degeneration, which suggested the existence of a quantitative relationship between the peripheral and central neural substrates of pain. Based on this observation, the purpose of the current study is to investigate the relationships among peripheral afferent fibers, brain responses to pain, and pain perception in healthy subjects. We combine skin biopsy (Lauria et al., 2010) and functional magnetic resonance imaging (fMRI) to measure the epidermal nerve fiber density (ENFD) of the distal leg and corresponding pain perception and brain activities after applying heat pain stimulation to the foot. We hypothesized that the neural correlates representing the quantity of cutaneous afferent nerves, particularly the posterior IC, would be parametrically associated with the functional network related to the perception of pain (i.e., the functional connectivity of the anterior IC).

## Methods

### Subjects

Seventeen healthy right-handed subjects (8 men and 9 women) between 26 and 70 years of age (mean: 48.5) participated in the study. Each subject's personal history of neurologic systems was taken to exclude latent neurologic disorders, and neurological examinations were performed to exclude any neuropsychiatric disorder or pain symptoms. Because clinically silent cerebrovascular pathology in persons of advanced age may affect neurovascular coupling and blood oxygen level-dependent (BOLD) signals (D'Esposito et al., 2003), subjects with the presence of cerebral infarcts, hemorrhage, or subcortical arteriosclerotic encephalopathy on T2 MRI were not enrolled in the current study. The study was approved by the Ethics Committee of National Taiwan University Hospital, Taipei, Taiwan. Informed consent was collected from all subjects before the experimental procedures.

### Quantification of epidermal nerve fiber density

Under local anesthesia with 2% lidocaine, a 3-mm punch of skin was taken from the distal leg 10 cm above the lateral malleolus. The immunohistochemical staining of skin tissues and quantification of ENFD followed previously established protocols (Tseng et al., 2006). Briefly, to visualize intraepidermal nerve fibers, protein gene product 9.5 (PGP 9.5; 1: 1000; UltraClone, Isle of Wight, England) immunostaining was performed on 50- $\mu$ m skin sections perpendicular to the dermis. PGP 9.5-immunoreactive nerve fibers in the epidermis were counted at a magnification of 400x with an Olympus BX40 microscope (Tokyo, Japan), and the length of the epidermis along the upper margin of the stratum corneum in each section was measured using Image-Pro PLUS (Media Cybernetics, Silver Spring, MD, USA). ENFD was therefore

expressed as the number of fibers per millimeter of epidermal length. For each skin tissue, there were 48–50 sections, and all of the sections were sequentially labeled. Every fifth section was immunostained and quantified. The mean value of these sections was considered the ENFD of the specimen. In our laboratory, the normative values [mean  $\pm$  SD (5th percentile)] of ENFD in the distal leg were  $11.16 \pm 3.70$  (5.88) fibers/mm for subjects aged <60 years and  $7.64 \pm 3.08$  (2.50) fibers/mm for subjects aged  $\geq 60$  years. The cutoff point for ENFD was 5.88 and 2.50 fibers/mm in the two age groups, respectively (Tseng et al., 2006).

### Thermal stimulation

An MR-compatible contact heat-evoked potential stimulator (PATHWAY sensory evaluation system; Medoc, Ramat Yishai, Israel) with a 27-mm-diameter circular thermofoil (572 mm<sup>2</sup>) was used to apply thermal stimulation (Tseng et al., 2013b). The thermofoil permitted a very rapid heating rate (up to 70 °C/s) and a fast cooling rate (up to 40 °C/s). Cooling began immediately after the thermode reached its target temperature. In this study, the stimulus temperature was defined as the temperature of the thermofoil applied to the skin.

### Experimental paradigm

The fMRI study was performed either before the skin biopsy or 7 days after it. None reported pain from the skin biopsy wound at the time of scanning. The block-designed fMRI paradigm was similar to our previous protocols (Tseng et al., 2013b). One hour before fMRI scanning, subjects familiarized themselves with the instructions for the experiment and the rating procedure in a waiting room. The imaging session consisted of one T2-weighted imaging, one T1-weighted anatomical scan, and one EPI run. To avoid pain from the skin biopsy wound and because the ENFDs at different anatomical sites on a lower limb were highly correlated in each individual (McArthur et al., 1998), the thermode was strapped to a fixed site on the dorsum of the right foot without causing any pressure to apply stimuli during the functional scan. The EPI run consisted of 5 presentations of the same stimulus that increased from the baseline 32 °C (36 s) to 44 °C (12 s) at 20 °C/s and then immediately returned to the baseline temperature at 40 °C/s after the thermode reached its target temperature. Throughout the imaging session, subjects were instructed to keep their eyes closed during stimulation, to refrain as much as possible from moving, to pay attention to the stimuli, and to keep in mind the sensation that they felt and report it after each functional scan was completed. To minimize the confounding effects of rating-related cognitive activity on pain perception (Bantick et al., 2002; Kong et al., 2006), subjects were asked to verbally rate the average perception for the 5 stimuli. To measure perceived pain intensity, we used a verbal rating scale (VRS) ranging from 0 to 10, with 0 indicating no sensation, 4 just barely painful, and 10 unbearable pain (Ochsner et al., 2006).

### fMRI data acquisition

All images were collected using a 3 T MRI scanner (Trio, Siemens, Erlangen, Germany). The subject's head was comfortably positioned inside a receive-only, 8-channel head coil that was padded with sponges, and the head was fixed with a strap across the forehead to minimize head motion. Each subject was provided with earplugs to minimize scanner noise. A whole-brain structural image was acquired using T1-weighted image (TR = 581 ms; TE = 6.7 ms; flip angle = 87°; field of view = 25  $\times$  25 cm; slice thickness = 3.9 mm; 35 slices in axial plane; acquisition matrix = 256  $\times$  256). Blood oxygenation level-dependent (BOLD) signals were acquired using a gradient-echo echoplanar imaging (EPI) sequence (TR = 3000 ms; TE = 30 ms; flip angle = 90°; field of view = 250  $\times$  250 mm; slice thickness = 3.9 mm; acquisition matrix = 64  $\times$  64; voxel size = 3.9  $\times$  3.9  $\times$  3.9 mm). A total

of 35 horizontal slices along the anterior/posterior commissure line were obtained, which covered the entire brain. The first 4 volumes were discarded to allow for spin saturation effects.

#### fMRI data analysis

fMRI data processing and analysis were performed using SPM8 ([www.fil.ion.ucl.ac.uk/spm](http://www.fil.ion.ucl.ac.uk/spm)) implemented in MATLAB (Mathworks, Sherborn, MA, USA). Briefly, the fMRI data series were realigned to the first volume in each scan sequence and re-sliced with sinc interpolation to correct for motion artifacts. Subjects who were enrolled in the present study had no scans with sudden head movements greater than 2 mm. The resulting mean image was registered to the corresponding T1-weighted anatomical image. To enable inter-subject analysis, the T1-weighted image of each subject was normalized to the standard Montreal Neurological Institute (MNI) template (Collins et al., 1994), and the normalization parameters were then applied to the functional data of that subject. The resampled voxel volume of the normalized images was  $2 \times 2 \times 2$  mm. Subsequently, data were smoothed using an isotropic Gaussian kernel with an 8 mm full width at half maximum (FWHM). A high-pass filter with a cutoff period of 128 s was used to remove low-frequency noise.

To identify voxels whose BOLD signals were significantly associated with the experimental paradigms, a general linear model (Friston et al., 1995b) was employed to model the two temporally discrete responses representing each stimulus temperature (i.e., 44 °C and 32 °C). These two regressors were obtained by convolving a boxcar sequence with the hemodynamic response function implemented in SPM (Friston et al., 1995a). Pain-specific effects were examined by evaluating the contrasts of the parameter estimates between the two regressors (i.e., 44 °C > 32 °C), which produced a *t* statistic for each voxel. The first-level *t*-contrasts from each subject were then entered into a second-level random-effects group analysis (Holmes and Friston, 1998).

The rationale of the analysis in the current study was as follows. First, we confirmed brain activations that are typically associated with pain to 44 °C stimuli using a one-sample *t*-test model in SPM. Activated areas from this group analysis were defined as pain-related brain regions in the current study. Second, to isolate the contribution of epidermal nerves to fMRI activations during painful stimulation without bias, a multiple linear regression analysis was conducted, using brain activations to 44 °C stimuli as dependent variable and individual ENFD values as independent variables, regressing out the effects of age (Tseng et al., 2013b), gender (Greenspan et al., 2007) and difference in VRS ratings (Peyron et al., 2000). For this analysis, a whole-brain exploratory investigation was followed by small-volume correction analyses in regions of interest, which included the thalamus, periaqueductal gray (PAG), and rostral ventromedial medulla (RVM). These regions were selected because previous studies have shown heavy projections of nociceptive spinothalamic tracts to these brain areas (Craig, 2003; Dum et al., 2009; Willis et al., 2001). In the third part of our analysis, we aimed to identify brain areas associated with pain perception. For this purpose, we conducted a whole-brain linear regression analysis in SPM, using VRS ratings as independent variables to detect brain activity correlated with pain intensity ratings. To further confirm that the ENFD values and VRS ratings were correlated with the BOLD signals in different portions of the IC, we employed another multiple linear regression analysis in SPM, using both ENFD values and VRS ratings as predictors and the BOLD signal in the left IC as the dependent variable. Fourth, to clarify whether anterior IC-related circuitry served as the neural basis of pain perception, we performed a psychophysiological interaction (PPI) analysis with a subsequent linear regression model to identify pain perception-related functional connectivity (described below). We hypothesized that the anterior IC interacted with other pain-related brain regions during painful stimulation to reflect perceived pain intensity and thus chose the bilateral anterior ICs as seed in PPI analysis because (1) it is the most frequently activated brain region in functional

imaging studies of pain (Apkarian et al., 2005), (2) it has been shown to have a crucial integrative role in the awareness of interoceptive information such as pain (Craig, 2009), and (3) its activity has been demonstrated to parallel pain ratings in the present report (see Results and Fig. 4) and previous studies (Coghill et al., 1999; Tseng et al., 2013b). To confirm that the identified regions were pain-related, a conjunction analysis was conducted on the results obtained from this linear regression analysis of PPI contrasts and the one-sample *t*-test that identified pain-related brain regions. Finally, because our main aim concerned the relationship between cutaneous afferent nerves and pain perception, we hypothesized that the neural circuitry underpinning this relationship should be correlated with both ENFD values and VRS ratings. Given that our PPI analyses demonstrated a positive correlation between pain perception and the functional connectivity from the anterior IC to SI, dorsomedial prefrontal cortex (PFC), and occipital cortex (see Results and Fig. 6), we thus examined whether the strength of the functional connectivity in these areas was also correlated with ENFD values. To this end, small-volume correction analyses in SI, dorsomedial PFC, and occipital cortex on the PPI analysis using ENFD values as a covariate were performed. To ascertain a spatial overlap of SI clusters whose connectivity with the anterior IC paralleled both VRS and ENFD, we performed small-volume correction analyses within the contralateral SI in both the linear regression analysis of PPI contrasts using VRS ratings as a covariate and the linear regression analysis of PPI contrasts using ENFD values as a covariate. This was followed by a conjunction analysis using the results of both analyses.

The statistical threshold for group statistical maps was a cluster size with at least 792 mm<sup>3</sup> and a voxelwise threshold of  $p = 0.001$ , which achieved an  $\alpha$  value of 0.05 after correcting for multiple comparisons. This threshold was based on the results of the Monte Carlo simulation ( $n = 10000$ ) (Forman et al., 1995) implemented in the 3dClustSim program of the Analysis of Functional Neuroimages software package (AFNI; <http://afni.nimh.nih.gov/afni/>), where the correction for multiple comparisons was confined within the brain mask (1547296 mm<sup>3</sup>) that was obtained from the analysis of average group activation maps in SPM8 (Tseng et al., 2013b). Small-volume correction analyses were performed using an initial height threshold of  $p < 0.005$ , uncorrected with subsequent family-wise error (FWE) correction for multiple comparisons at a level of  $p < 0.05$ . Considering somatotopy in SI, the definition of the region of interest (ROI) for the foot area in this region, i.e., a sphere with a 12-mm radius centered on MNI coordinates  $x/y/z = -12/-39/64$  for the left SI, was based on previous fMRI studies applying painful heat stimuli to the foot (Bingel et al., 2004). According to a meta-analysis of painful heat-related activation (Duerden and Albanese, 2013), the ROI of the left thalamus was defined as a 12-mm sphere centered at MNI coordinates  $x/y/z = -16/-20/12$ . ROIs of the PAG ( $0/-32/-10$ ) and RVM ( $-2/-36/-40$ ) were defined as spheres with a radius of 6 mm based on previous brainstem fMRI studies on pain (Eippert et al., 2009; Fairhurst et al., 2007). In the current study, we used the automated anatomical labeling ROI library in the SPM MarsBar toolbox (Tzourio-Mazoyer et al., 2002) to define the anterior (with an MNI *y*-coordinate > 0) and posterior (with an MNI *y*-coordinate < 0) portion of insula, dorsomedial PFC, and occipital cortex. All stereotactic coordinates are reported in MNI space (<http://mni.mcgill.ca/>). For each subject, the mean BOLD signal change of the fMRI data and the parameter estimates in brain regions showing significant PPI effects were extracted from each ROI using the MarsBar toolbox (<http://marsbar.sourceforge.net/>) (Brett et al., 2002).

#### PPI analysis

To investigate whether painful stimulation altered patterns of functional connectivity, we performed functional connectivity analyses using a generalized form of a context-dependent PPI method (<http://www.nitrc.org/projects/gppi>) (McLaren et al., 2012). This analysis assesses context-dependent interactions of brain regions by examining

temporal correlations between BOLD signals of different brain areas that were significantly changed with the experimental conditions (Friston et al., 1997). We extracted the deconvolved time series of activity averaged over the seed region (i.e., the bilateral anterior ICs and bilateral posterior ICs) in each subject. The regressors in the PPI analysis included (1) a vector representing the contrast of tasks (1 for painful 44 °C stimulation; –1 for painless 32 °C stimulation) (the psychological regressor), (2) a regressor representing the activation time course of the seed region (the physiological variable), and (3) a PPI regressor representing the cross product of the previous two. To identify brain regions in which the degree of functional coupling with the anterior IC during painful stimulation reflected the perception of pain or ENFD, first-level PPI contrasts were entered into second-level linear regression analyses using individual VRS ratings or ENFD values as the covariate.

### Statistical analysis

Statistical analyses were conducted using SPSS (Chicago, IL, USA) and GraphPad Prism (GraphPad Software, San Diego, CA, USA). Continuous variables following a Gaussian distribution were expressed as the mean  $\pm$  standard deviation. Pearson's correlation test was employed to assess the linear relationship between two variables. Analysis of covariance (ANCOVA) was employed to test whether slopes of linear regression lines were significantly different (Fig. 3).

## Results

### Epidermal nerves and psychophysical data

In the skin of healthy subjects, cutaneous afferents of the small fiber type, arising from the dermis, terminated in the epidermis with varicose appearance (Fig. 1). The abundance of epidermal nerve fibers varied among different subjects and ENFD served as a quantitative measure. In the current study, the ENFD values for all of the recruited subjects were within the normal limits (Table 1). On average, subjects felt moderate pain sensation at the 44 °C stimulation (mean  $\pm$  SD for VRS ratings, 6.8  $\pm$  1.8). Individual ENFD values did not correlate directly with the corresponding VRS ratings to painful stimuli ( $p = 0.090$ ).

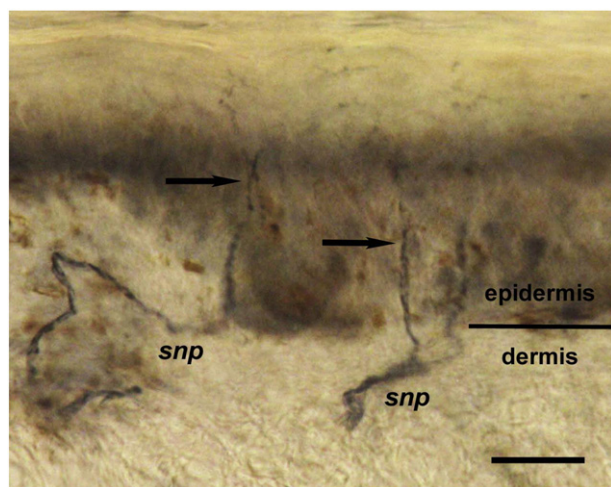


**Fig. 1.** Sensory nerve fibers in the skin. Skin sections from healthy subjects were immunostained with anti-protein gene product 9.5, which labels sensory nerve terminals in the skin. Epidermal nerve fibers (arrows) arose from nerve fibers in the subepidermal nerve plexus (snp) of the dermis and entered the epidermis vertically with a varicose appearance (scale bar = 20  $\mu$ m).

**Table 1**

Epidermal nerve fiber density (ENFD) of the distal leg and ratings from the verbal rating scale (VRS) in our subjects.

Subject no	Age (year)	Gender	ENFD (fibers/mm)	VRS
1	26	F	13.17	9
2	26	F	9.6	7
3	27	M	9.11	7
4	32	M	11.92	6
5	32	M	11.75	9
6	43	M	8.59	7
7	44	M	6.42	7
8	47	F	7.89	7
9	49	F	9.53	4
10	50	F	7.21	9
11	56	F	11.79	10
12	59	F	7.63	5
13	64	F	7.06	4
14	64	F	4.37	7
15	66	M	4.59	4
16	69	M	5.45	8
17	70	M	5.72	6

### Epidermal nerves and fMRI signals

As observed in Fig. 2 and Supplementary Table 1, painful 44 °C stimuli evoked brain activations in typical pain-related regions, which included the SI, secondary somatosensory cortex, IC, ACC, PFC, and thalamus (Apkarian et al., 2005). This result thus validated our paradigms.

To further explore the significance of epidermal nerves, we examined if the quantity of epidermal nerves was associated with the brain activity to pain. Because age (Tseng et al., 2013b), gender (Greenspan et al., 2007), and individual pain intensity ratings (Peyron et al., 2000) potentially biased brain responses to pain, we included these factors in addition to the ENFD values in a whole-brain multiple linear regression model in SPM to isolate activity that was unbiasedly correlated with the quantity of epidermal nerves. Consistent with our hypothesis, this analysis indicated that only the activity in the contralateral posterior IC was significantly associated with ENFD values across the entire brain (Fig. 3A; Table 2). Moreover, small-volume correction analyses

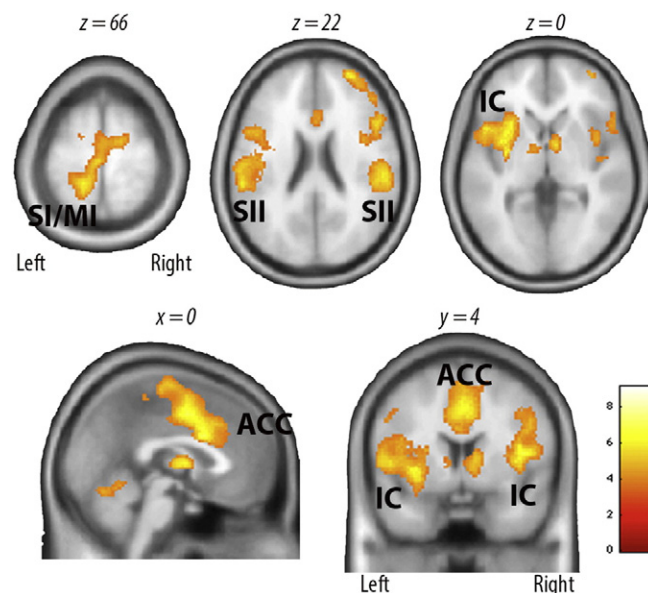


**Fig. 2.** Brain regions activated to heat pain stimulation. In this whole-brain analysis, activations to 44 °C stimulation are illustrated at  $p < 0.001$ , with an extent threshold of 792 mm<sup>3</sup> (see Materials and Methods) and overlaid on an average structural image. The bar on the right side shows the range of  $t$  scores for SPM8. ACC, anterior cingulate cortex; IC, insular cortex; MI, primary motor cortex; SI, primary somatosensory cortex; SII, secondary somatosensory cortex.

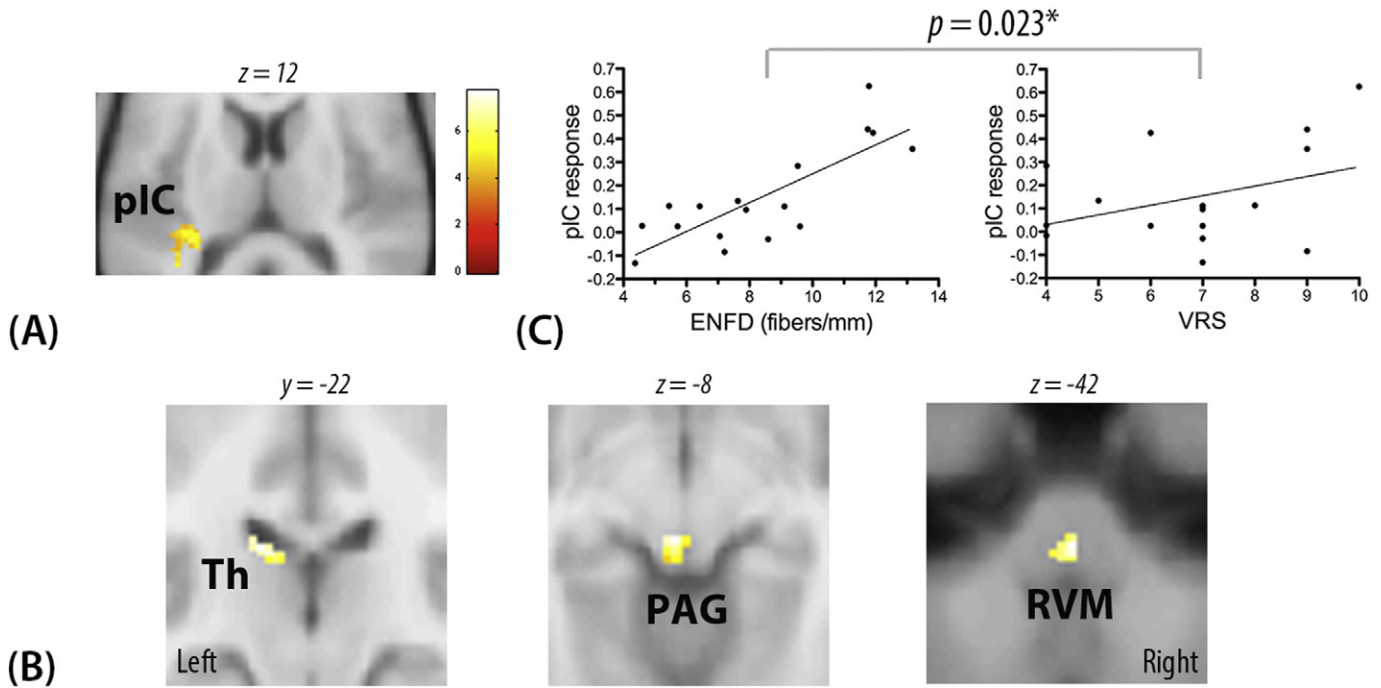


**Fig. 3.** BOLD signals correlated with epidermal nerve fiber density. Functional magnetic resonance imaging signals to thermal pain stimuli that were positively predicted by epidermal nerve fiber density (ENFD) are overlaid on an average structural image. Analyses across the whole brain (A) and in regions of interest ( $p < 0.05$ , small-volume corrected) (B) are displayed. The plot in C shows that the correlation between activity in the posterior insular cortex (pIC) and ENFD values was significantly stronger than the correlation between pIC activity and ratings from the verbal rating scale (VRS) (analysis of covariance,  $F_{(1,30)} = 5.76$ ,  $p = 0.023$ ). The bar on the right side in A shows the range of  $t$  scores for SPM8. The image data in B are thresholded for display at  $p < 0.005$  uncorrected. \* $p < 0.05$  by an analysis of covariance. Th, thalamus; PAG, periaqueductal gray; RVM, rostral ventromedial medulla.

restricted to the ROIs showed that brain responses in the thalamus, PAG, and RVM were also positively correlated with ENFD values (Fig. 3B; Table 2).

#### Pain perception and fMRI signals

Because the anterior part of the insula has a crucial role in the awareness of pain perception (Craig, 2009), we first confirmed that the anterior IC was associated with pain perception. As shown in Fig. 4 and Table 3, in a simple regression model in SPM using VRS scores as a covariate, the pain intensity ratings were positively correlated with the BOLD signal in the anterior IC, SI, secondary somatosensory cortex, and ACC.

The above findings suggested that different insular subregions were associated with ENFD values (the posterior IC) and VRS ratings (the anterior IC). Because different parts of the insula may play different roles in pain processing (Baliki et al., 2009; Craig, 2009), we further clarified

**Table 2**  
Brain activity correlated with epidermal nerve fiber density.

Region	Side	MNI coordinates (x, y, z)	t value	p value	Correlation with VRS	
					r	p value
pIC	Left	-38, -12, -8	8.28	<0.001	0.276	0.283
		-34, -30, 12	5.37	<0.001		
Thalamus	Left	-12, -22, 18	4.20	0.001*	0.189	0.468
PAG	Left	-2, -28, -8	5.29	<0.001*	0.195	0.453
RVM	Right	2, -34, -42	4.66	<0.001*	0.158	0.546

The table shows the anatomical locations, MNI coordinates,  $t$  scores, and uncorrected  $p$  values of peak voxels. The right panel shows the correlation coefficients and  $p$  value of the linear regression between the BOLD signal in activated clusters and the ratings from the verbal rating scale (VRS). Based on a Monte Carlo simulation, only voxels surviving a threshold of  $p < 0.001$  uncorrected with an extent size of  $792 \text{ mm}^3$  are reported. See Materials and Methods for details. PAG, periaqueductal gray; pIC, posterior insular cortex; RVM, rostral ventromedial medulla.

\* Small-volume corrections with family-wise error correction of  $p < 0.05$ .

whether the BOLD signals in the anterior and posterior insula were predicted by ENFD values and VRS ratings, respectively. By conducting a multiple linear regression analysis using ENFD values and VRS ratings as covariates and performing small-volume correction analyses in the IC, our results confirmed that the BOLD signal in the posterior IC was predicted by ENFD values rather than VRS ratings, whereas activity in the anterior IC was parametrically associated with VRS ratings but not

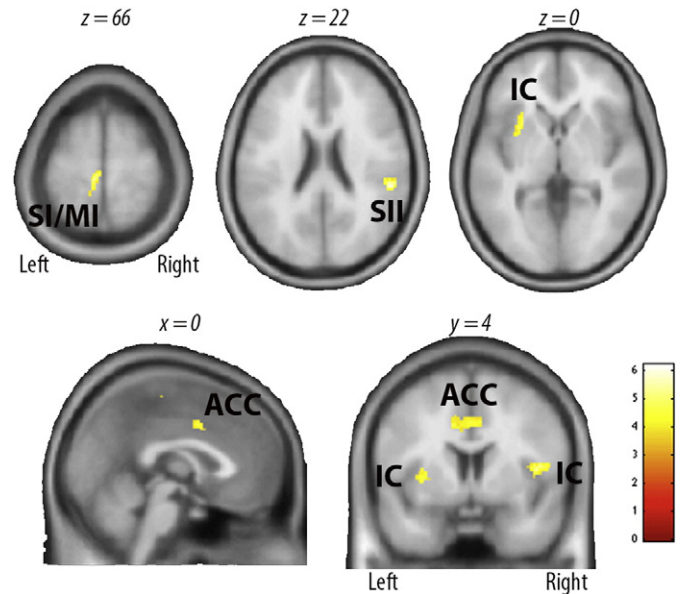


**Fig. 4.** BOLD signals correlated with pain perception. In a whole-brain inter-subject linear regression analysis of functional magnetic resonance imaging data, regional responses to thermal pain stimuli that were positively correlated with ratings from the verbal rating scale are overlaid on an average structural image. The bar on the right side shows the range of  $t$  scores for SPM8. ACC, anterior cingulate cortex; IC, insular cortex; MI, primary motor cortex; SI, primary somatosensory cortex; SII, secondary somatosensory cortex.

**Table 3**

Brain activity correlated with the perception of pain.

Region	Side	MNI coordinates (x, y, z)	t value	p value	Correlation with ENFD	
					r	p value
IC	Left	−32, 12, −10	5.24	<0.001	0.405	0.107
	Right	44, 2, 10	6.20	<0.001	0.524	0.275
SI	Left	−10, −42, 66	3.90	0.001	0.138	0.599
MI	Left	−6, −30, 66	5.31	<0.001	0.323	0.207
SII	Right	54, −34, 22	5.94	<0.001	0.440	0.077
ACC	Left	0, 4, 40	4.61	<0.001	0.241	0.351

The table shows the anatomical locations, MNI coordinates, *t* scores, and uncorrected *p* values of peak voxels. The right panel shows the correlation coefficients and *p* values of the linear regression between the BOLD signal in activated clusters and the epidermal nerve fiber density (ENFD) values. Based on a Monte Carlo simulation, only voxels surviving a threshold of  $p < 0.001$  uncorrected with an extent size of 792 mm<sup>3</sup> are reported. ACC, anterior cingulate cortex; IC, insular cortex; MI, primary motor cortex; SI, primary somatosensory cortex; SII, secondary somatosensory cortex.

with ENFD values (Fig. 5). In line with this finding, the BOLD signals in brain areas whose activities covaried with ENFD values were not correlated with VRS ratings (Table 2), and vice versa (Table 3). Moreover, the correlation between activity in the posterior IC and ENFD values was significantly different from the correlation between posterior IC activity and VRS ratings (ANCOVA,  $F_{(1,30)} = 5.76$ ,  $p = 0.023$ ) (Fig. 3C), strongly suggesting that ENFD values specifically contributed to the response in the posterior IC.

Given that evidence points toward functional interplay between the anterior IC and other pain-related brain areas during pain processing (Peltz et al., 2011; Wiech et al., 2010), we performed a PPI analysis to examine if the bilateral anterior ICs were functionally linked with other pain-processing areas during painful stimulation to substantiate pain perception. A whole-brain analysis revealed a correlation of VRS ratings with the coupling between the anterior IC and contralateral SI, dorsomedial PFC, and occipital cortex (Fig. 6, Table 4). A conjunction analysis proved that the clusters in the SI and PFC overlapped with the pain-related brain regions described above (Supplementary Fig. 1), thus supporting our hypothesis that the coupling between the anterior

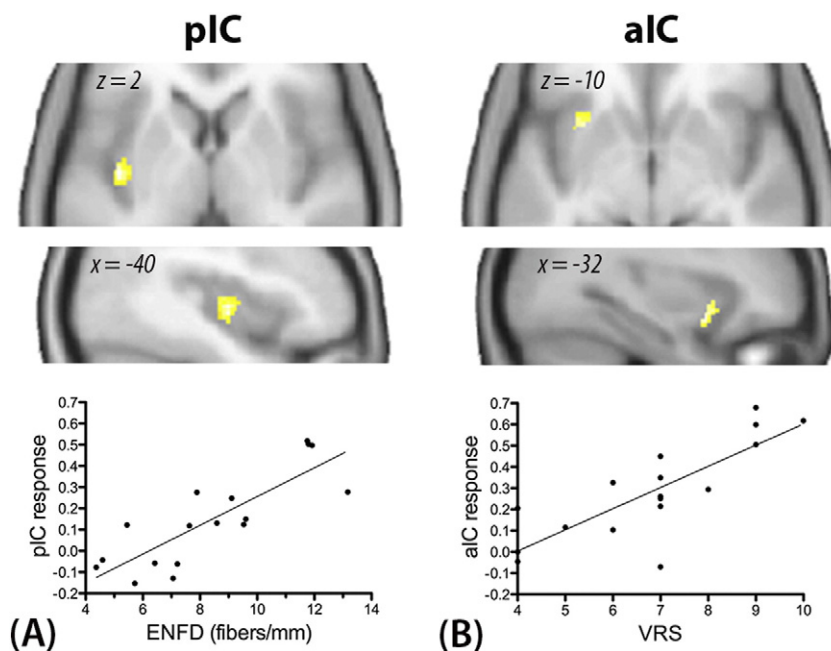


**Fig. 5.** Insular activity specifically predicted by epidermal nerve fiber density (ENFD) values and ratings from the verbal rating scale (VRS). In a multiple linear regression analysis using ENFD values and VRS ratings as predictors, BOLD signals in the left insula ( $p < 0.05$ , small-volume corrected) to thermal pain stimuli that were positively predicted by ENFD values (Montreal Neurological Institute [MNI] peak coordinates =  $-40/-8/2$ ;  $t$  value = 4.79) (A) or VRS ratings (MNI peak coordinates =  $-32/12/-10$ ;  $t$  value = 4.43) (B) are overlaid on an average structural image. The plots below illustrate positive correlations (1) between ENFD values and activity in the posterior insular cortex (pIC) (A) and (2) between VRS ratings and activity in the anterior insular cortex (aIC) (B). The image data are thresholded for display at  $p < 0.005$ , uncorrected.

## Functional coupling

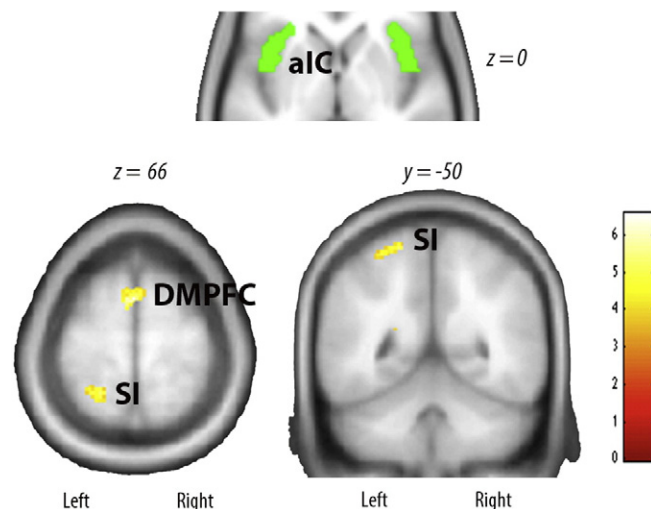


**Fig. 6.** Functional connectivity correlated with pain perception. A whole-brain psychophysical interaction analysis using the bilateral anterior insular cortices (aIC) (green) as the seed showed that the functional synchrony between the aIC and the primary somatosensory cortex (SI) as well as the dorsomedial prefrontal cortex (DMPPFC) during painful stimulation paralleled pain intensity ratings. The bar on the right side shows the range of *t* scores for SPM8.

IC and pain-related brain regions underlay pain perception. By contrast, another PPI analysis using the bilateral posterior ICs as the seed did not identify any significant functional connectivity that paralleled pain perception.

### Epidermal nerves and pain perception

The main focus of the present study is to elucidate the relationship between peripheral afferents and pain perception. We hypothesized that the neural responses mediating this relationship should be

**Table 4**  
Functional connectivity associated with the perception of pain.

Region	Side	MNI coordinates (x, y, z)	t value	p value
SI	Left	−20, −50, 66	5.10	<0.001
DMPFC	Left	0, 6, 66	5.58	<0.001
OC	Left	−12, −62, 10	5.28	<0.001

The table shows the anatomical locations, MNI coordinates, *t* scores, and uncorrected *p* values of peak voxels. Bilateral anterior insular cortices were selected as the seed region in the psychophysical interaction analysis. Based on a Monte Carlo simulation, only voxels surviving a threshold of  $p < 0.001$ , uncorrected with an extent size of  $792 \text{ mm}^3$  are reported. DMPFC, dorsomedial prefrontal cortex; OC, occipital cortex; SI, primary somatosensory cortex.

correlated with both ENFD values and VRS ratings. If the pain perception-related functional circuitry identified above (Fig. 6) integrated information about stimulus intensity that was conveyed via cutaneous primary afferents, it would be associated with the quantity of epidermal innervation. To prove this hypothesis, we performed small-volume correction analyses in the SI, dorsomedial PFC, and occipital cortex on the above-mentioned PPI analyses. Importantly, only the functional connectivity from the anterior IC to the SI exhibited a significant correlation with ENFD values (Fig. 7A). Another conjunction analysis using anterior IC-SI connectivity associated with VRS ratings (Fig. 6) and ENFD values (Fig. 7A) confirmed a spatial overlap (Supplementary Fig. 1). In addition to ENFD, the strength of anterior IC-SI coupling also covaried with ENFD-related brain activity, i.e., the BOLD signal in the left posterior IC (Fig. 7B).

The interrelationships among pain perception, anterior IC-SI coupling, activity in the left posterior IC, and skin innervation were illustrated in Fig. 8, in which the mean BOLD signal change in the left posterior IC and the parameter estimates representing the strength of the anterior IC-SI coupling were extracted and correlated with the ENFD values and VRS ratings. Taken together, these findings strongly suggested that the functional coupling between the anterior IC and SI underlay the relationship between skin innervation and pain perception.

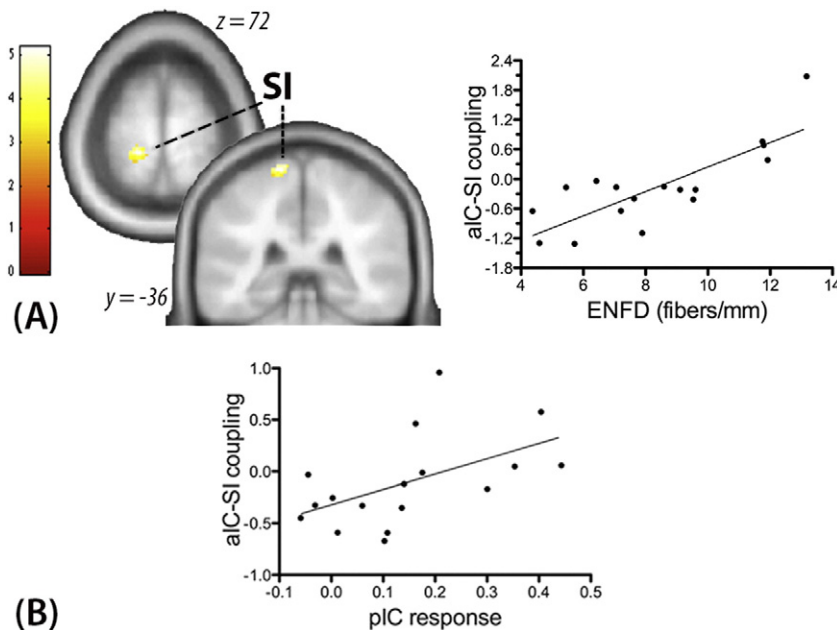


**Fig. 7.** The relationship between skin innervation and functional connectivity related to pain perception. (A) A psychophysical interaction analysis using the bilateral anterior insular cortices (aIC) as the seed showed that, during painful stimulation, the functional coupling between the aIC and the primary somatosensory cortex (SI) ( $p < 0.05$ , small-volume corrected), which has already been shown to parallel pain intensity ratings (see Fig. 6), was correlated with epidermal nerve fiber density (ENFD) values. The image data are overlaid on an average structural image and are thresholded for display at  $p < 0.005$ , uncorrected. The bar on the left side shows the range of *t* scores for SPM8. The plot on the right illustrates that the larger the ENFD value, the stronger the aIC-SI coupling during painful stimulation. (B) The BOLD signal in the left posterior insular cortex (pIC), which paralleled the ENFD values (see Fig. 3A), also correlated with the strength of the aIC-SI connectivity (slope =  $1.481 \pm 0.623$ ,  $r = 0.524$ ,  $p = 0.031$ ).

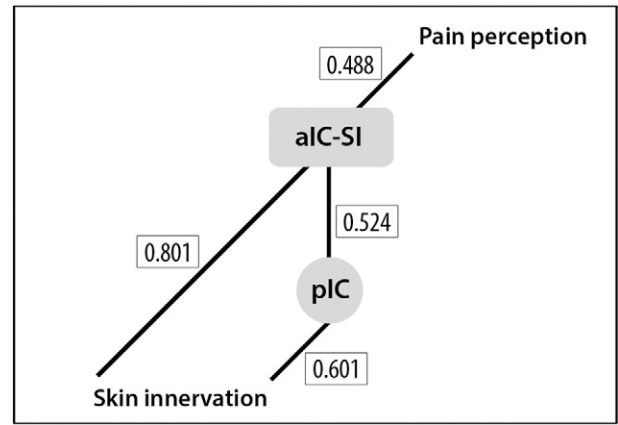


**Fig. 8.** Neural substrates underlying the relationship between cutaneous afferent nerves and pain perception. Pain perception is represented by the functional connectivity between the anterior insular cortex (aIC) and the primary somatosensory cortex (SI) (identified in a whole-brain analysis in SPM8; see Fig. 6), which is parametrically associated with epidermal nerve fiber density (ENFD) values and activity in ENFD-associated brain region, i.e., the posterior insular cortex (pIC) (identified in a whole-brain analysis in SPM8; see Fig. 3A). Black lines represent significant pair-wise correlations ( $p < 0.05$ ) using Pearson's correlation tests. Numbers in the rectangles indicate the pair-wise correlation coefficients.

## Discussion

Cutaneous primary afferents consist of C and A $\delta$  fibers (Kennedy and Wendelschafer-Crabb, 1993). Although they are correlated with the perception of innocuous heat in healthy subjects (Pan et al., 2001), a gap exists between these small-diameter afferents and the sensation of pain. The current study investigated the coupling of the small-diameter primary afferent fibers evaluated by using skin biopsy on the perception of heat pain and analyzing pain-evoked fMRI signals. The results indicate that, along the pain pathway, the degree of cutaneous innervation was correlated with brain responses in the posterior IC,

thalamus, PAG, and RVM. Activity in these regions and the abundance of skin innervation itself did not covary with the perception of pain. Instead, the quantity of epidermal nerves and the response in the posterior IC to pain were correlated with the functional coupling between the anterior IC and SI, which was parametrically associated with pain perception. The current study suggests that when we perceive the intensity of heat pain stimulation, the anterior IC interacts with the SI to integrate information about stimulus intensity conveyed via peripheral afferent fibers.

#### *The functional activity associated with epidermal nerves*

In contrast to a variety of studies showing that the extent of cutaneous innervation was associated with pathological pain conditions (Lauria et al., 2010), little attention has been paid to delineate its relationship with acute experimental pain in healthy subjects. In the present study, fMRI data were regressed for the possible effects of age (Tseng et al., 2013b), gender (Greenspan et al., 2007) and pain intensity ratings (Peyron et al., 2000), and the responses in the posterior IC, thalamus, PAG, and RVM were significantly predicted by the quantity of ENFD. Anatomically, nociceptive spinothalamic neurons project to the RVM and PAG (Craig, 2003), both of which receive input from the amygdala, hypothalamus, and limbic neocortex to subservise the descending modulatory processing of painful stimulation (Todd and Koerber, 2013). Moreover, efferent fibers from the PAG enter the thalamus (Groenewegen, 1988), from which the posterior IC receives nociceptive inputs (Craig, 2003). Although these pathways are suggested to reflect the ongoing physiological responses to nociceptive stimulation (Craig, 2003), empirical evidence is lacking concerning the relationship between peripheral afferents and pain-related brain activity during pain processing in humans. Hence, our data not only establish the relationship between primary nociceptive afferents and pain-related brain regions but also substantiate the concept that a painful stimulus activates both the bottom-up pathway and the top-down pain modulatory regions in the brainstem, thereby achieving homeostatic control.

Of particular note is the posterior IC, the only brain region whose BOLD signals to pain correlated with ENFD in our whole-brain analysis. Indeed, this finding is in accordance with previous studies showing that the posterior IC receives the densest projections from the lamina I spinothalamicocortical pathway (Craig, 2003). This part of the insula contains nociceptive neurons (Robinson and Burton, 1980) and participates in processing the sensory-discriminative features of pain (Brooks et al., 2002; Treede et al., 1999), including the coding of objective thermal intensity (Bornhovd et al., 2002; Craig et al., 2000). Recent work has revealed that the posterior IC was responsive to physical pain rather than mental representations of pain stimuli (Fairhurst et al., 2012) and that its response was parametrically associated with the magnitude of noxious stimulation irrespective of its quality (Peltz et al., 2011). Direct electrical stimulation of this region in humans can elicit painful sensations (Ostrowsky et al., 2002; Mazzola et al., 2006). Clinically, lesions encroaching the posterior IC alter pain threshold (Garcia-Larrea et al., 2010; Greenspan et al., 1999; Schmähmann and Leifer, 1992). Taken together with our results, these observations suggest that the posterior IC serves as the primary representation of the nociceptive information in the cortex (Craig, 2009).

#### *Distinct roles of insular subregions in pain processing*

The lack of correlation between the extent of epidermal innervation and pain intensity ratings implies distinct neural substrates to subservise pain perception. This speculation was proved by our regression analysis, which showed that the activity in the anterior IC, somatosensory cortices, and cingulate cortex paralleled individual ratings of pain intensity. The dissimilarity between ENFD- and pain rating-correlated brain regions suggests that different central mechanisms are responsible for representing pain input and evoking painful sensation in the human

brain, with the former depending on both the brainstem, subcortical, and cortical structures and the latter relying primarily on the responses in cortical substrates.

Although both ENFD values and VRS ratings covaried with the BOLD signal in the IC, our analyses found that both factors predicted responses in distinct insular subregions. Different from the posterior IC, whose response was associated with the quantity of skin innervation, activity in the anterior IC was specifically predicted by subjective pain ratings. This result corroborates the structural connectivity of the insula, with the posterior IC receiving projections from nociceptive spinothalamic neurons (Craig, 2003; Dum et al., 2009; Willis et al., 2001) and its anterior counterpart connected with the PFC and limbic structures for associating with the awareness of interoceptive stimulation (Craig, 2009). Our observation also resonates with a previous study demonstrating distinct roles of different insular portions in thermal sensation, with the posterior IC coding for stimulus intensity and the anterior IC related to subjective stimulus perception (Craig et al., 2000). Thus, the insula potentially serves as the interface between the representation of nociceptive inputs and subjective pain perception (Baliki et al., 2009) during the processing of pain in the human brain.

#### *Functional connectivity related to pain perception*

The notion that the anterior and posterior insula have different roles in pain processing is further supported by our functional connectivity analyses. Compared with the painless baseline, the functional connectivity between the anterior IC and SI and PFC during painful stimulation paralleled the perception to pain. By contrast, no connectivity with the posterior IC was found to reflect subjects' feelings. In contrast to the pattern of structural and resting state connectivity of the insula (Wiech et al., 2014), these findings suggest a unique set of insular functional connectivity for processing perceived pain intensity, which is consistent with recent observations that the anterior IC couples with distinct pain-related brain regions to process pain (Peltz et al., 2011; Wiech et al., 2010). However, it remains unclear whether the functional connectivity of the anterior IC pertains to the perception of pain. Our data therefore clarify this issue by demonstrating that the anterior IC is the critical structure in determining pain perception. Although no substantial nociceptive spinothalamic neurons send nerve fibers to the anterior IC, they have been shown to project to the SI (Craig, 2003; Dum et al., 2009; Willis et al., 2001). The response to nociceptive stimulation in SI neurons depends largely on input from lamina I nociceptive neurons (Craig, 2003), and SI activity has been shown to strongly correlate with heat pain intensity (Coghill et al., 1999; Timmermann et al., 2001; Tseng et al., 2010). Moreover, the anterior IC is connected with the SI and projects to the PFC (Augustine, 1996; Cipolloni and Pandya, 1999). Given that the SI and medial PFC are putatively responsible for the sensory-discriminative and affective-cognitive dimensions of pain, respectively (Treede et al., 1999), the constellation of functional couplings between the anterior IC and both regions thus serves well to reflect the complex nature of pain. Unlike the posterior IC, damage to the anterior IC does not change pain sensitivity but results in pain asymbolia (Berthier et al., 1988; Greenspan et al., 1999). Taken together, our results indicate that the anterior IC couples with other pain-related brain regions to integrate information related to the multiple dimensions of pain into its perception.

#### *Relationships between epidermal nerves and pain perception*

Above all, our analyses not only demonstrated different central representations of skin innervation (i.e., activity in the posterior IC) and pain perception (i.e., anterior IC-SI connectivity) but also revealed correlations between anterior IC-SI connectivity and activity of the posterior IC, as well as the quantity of epidermal nerves. These relationships provide neuroimaging evidence for an indirect role of cutaneous afferent fibers in human pain perception. The correlations also substantiate

the notion that the neural circuitry subserving pain perception interacts with the neural substrate representing nociceptive fibers (Fig. 8). These cerebral modulation mechanisms explain why prior studies failed to find a direct correlation between skin innervation and the perception of pain (Herrmann et al., 2004; Selim et al., 2010; Zhou et al., 2007).

In conclusion, an integrated analysis of structures at both the peripheral and central levels substantially improves our understanding of the neural mechanisms of pain processing. Our study sheds light on a new research direction to unravel the underlying mechanisms of pain processing along the neural axis and provides a basis to investigate alterations in central nociceptive processing following peripheral nerve injury in future studies.

## Acknowledgments

We appreciate the support from the Ministry of Science and Technology (formerly the National Science of Council), Taiwan (101-2321-B-002-080, 102-2321-B-002-061 and 103-2321-B-002-030) and National Taiwan University Hospital (101C101-201).

## Appendix A. Supplementary data

Supplementary data to this article can be found online at <http://dx.doi.org/10.1016/j.neuroimage.2015.08.021>.

## References

- Apkarian, A.V., Bushnell, M.C., Treede, R.D., Zubieta, J.K., 2005. Human brain mechanisms of pain perception and regulation in health and disease. *Eur. J. Pain* 9, 463–484.
- Augustine, J.R., 1996. Circuitry and functional aspects of the insular lobe in primates including humans. *Brain Res. Brain Res. Rev.* 22, 229–244.
- Baliki, M.N., Geha, P.Y., Apkarian, A.V., 2009. Parsing pain perception between nociceptive representation and magnitude estimation. *J. Neurophysiol.* 101, 875–887.
- Bantick, S.J., Wise, R.G., Ploghaus, A., Clare, S., Smith, S.M., Tracey, I., 2002. Imaging how attention modulates pain in humans using functional MRI. *Brain* 125, 310–319.
- Berthier, M., Starkstein, S., Leiguarda, R., 1988. Asymbolia for pain: a sensory-limbic disconnection syndrome. *Ann. Neurol.* 24, 41–49.
- Bingel, U., Lorenz, J., Glauche, V., Knab, R., Glascher, J., Weiller, C., Buchel, C., 2004. Somatotopic organization of human somatosensory cortices for pain: a single trial fMRI study. *Neuroimage* 23, 224–232.
- Bornhovd, K., Quante, M., Glauche, V., Bromm, B., Weiller, C., Buchel, C., 2002. Painful stimuli evoke different stimulus-response functions in the amygdala, prefrontal, insula and somatosensory cortex: a single-trial fMRI study. *Brain* 125, 1326–1336.
- Brett, M., Anton, J.L., Valabregue, R., Poline, J.B., 2002. Region of interest analysis using an SPM toolbox. *Neuroimage* 16, 1141–1142.
- Brooks, J.C., Nurmikko, T.J., Bimson, W.E., Singh, K.D., Roberts, N., 2002. fMRI of thermal pain: effects of stimulus laterality and attention. *Neuroimage* 15, 293–301.
- Cipolloni, P.B., Pandya, D.N., 1999. Cortical connections of the frontoparietal opercular areas in the rhesus monkey. *J. Comp. Neurol.* 403, 431–458.
- Coghil, R.C., Sang, C.N., Maisog, J.H., Iadarola, M.J., 1999. Pain intensity processing within the human brain: a bilateral, distributed mechanism. *J. Neurophysiol.* 82, 1934–1943.
- Collins, D.L., Neelin, P., Peters, T.M., Evans, A.C., 1994. Automatic 3D intersubject registration of MR volumetric data in standardized Talairach space. *J. Comput. Assist. Tomogr.* 18, 192–205.
- Craig, A.D., 2003. Pain mechanisms: labeled lines versus convergence in central processing. *Annu. Rev. Neurosci.* 26, 1–30.
- Craig, A.D., 2009. How do you feel—now? The anterior insula and human awareness. *Nat. Rev. Neurosci.* 10, 59–70.
- Craig, A.D., Chen, K., Bandy, D., Reiman, E.M., 2000. Thermosensory activation of insular cortex. *Nat. Neurosci.* 3, 184–190.
- D'Esposito, M., Deouell, L.Y., Gazzaley, A., 2003. Alterations in the bold fMRI signal with ageing and disease: a challenge for neuroimaging. *Nat. Rev. Neurosci.* 4, 863–872.
- Duerden, E.G., Albanese, M.C., 2013. Localization of pain-related brain activation: a meta-analysis of neuroimaging data. *Hum. Brain Mapp.* 34, 109–149.
- Dum, R.P., Levinthal, D.J., Strick, P.L., 2009. The spinothalamic system targets motor and sensory areas in the cerebral cortex of monkeys. *J. Neurosci.* 29, 14223–14235.
- Eippert, F., Bingel, U., Schoell, E.D., Yacubian, J., Klingler, R., Lorenz, J., Buchel, C., 2009. Activation of the opioidergic descending pain control system underlies placebo analgesia. *Neuron* 63, 533–543.
- Fairhurst, M., Wiech, K., Dunckley, P., Tracey, I., 2007. Anticipatory brainstem activity predicts neural processing of pain in humans. *Pain* 128, 101–110.
- Fairhurst, M., Fairhurst, K., Berna, C., Tracey, I., 2012. An fMRI study exploring the overlap and differences between neural representations of physical and recalled pain. *PLoS One* 7, e48711.
- Forman, S.D., Cohen, J.D., Fitzgerald, M., Eddy, W.F., Mintun, M.A., Noll, D.C., 1995. Improved assessment of significant activation in functional magnetic resonance imaging (fMRI): use of a cluster-size threshold. *Magn. Reson. Med.* 33, 636–647.
- Friston, K.J., Frith, C.D., Turner, R., Frackowiak, R.S.J., 1995a. Characterizing evoked hemodynamics with fMRI. *Neuroimage* 2, 157–165.
- Friston, K.J., Holmes, A.P., Worsley, K.J., Poline, J.P., Frith, C.D., Frackowiak, R.S., 1995b. Statistical parametric maps in functional imaging: a general linear approach. *Hum. Brain Mapp.* 2, 189–210.
- Friston, K.J., Buechel, C., Fink, G.R., Morris, J., Rolls, E., Dolan, R.J., 1997. Psychophysiological and modulatory interactions in neuroimaging. *Neuroimage* 6, 218–229.
- Garcia-Larrea, L., Perchet, C., Creach, C., Convers, P., Peyron, R., Laurent, B., Mauguere, F., Magnin, M., 2010. Operculo-insular pain (parasympathetic pain): a distinct central pain syndrome. *Brain* 133, 2528–2539.
- Greenspan, J.D., Lee, R.R., Lenz, F.A., 1999. Pain sensitivity alterations as a function of lesion location in the parasympathetic cortex. *Pain* 81, 273–282.
- Greenspan, J.D., Craft, R.M., LeResche, L., Arendt-Nielsen, L., Berkley, K.J., Fillingim, R.B., Gold, M.S., Holdcroft, A., Lautenbacher, S., Mayer, E.A., Mogil, J.S., Murphy, A.Z., Traub, R.J., Consensus Working Group of the Sex, G., Pain, S.I.G.o.t.I., 2007. Studying sex and gender differences in pain and analgesia: a consensus report. *Pain* 132 (Suppl. 1), S26–S45.
- Groenewegen, H.J., 1988. Organization of the afferent connections of the mediodorsal thalamic nucleus in the rat, related to the mediodorsal-prefrontal topography. *Neuroscience* 24, 379–431.
- Herrmann, D.N., McDermott, M.P., Henderson, D., Chen, L., Akowuah, K., Schiffitto, G., North East, A.D.C., 2004. Epidermal nerve fiber density, axonal swellings and QST as predictors of HIV distal sensory neuropathy. *Muscle Nerve* 29, 420–427.
- Holmes, A.P., Friston, K.J., 1998. Generalisability, random effects and population inference. *Neuroimage* 7, S74.
- Hsieh, P.C., Tseng, M.T., Chao, C.C., Lin, Y.H., Tseng, W.Y., Liu, K.H., Chiang, M.C., Hsieh, S.T., 2015. Imaging signatures of altered brain responses in small-fiber neuropathy: reduced functional connectivity of the limbic system after peripheral nerve degeneration. *Pain* 156 (5), 904–916.
- Kennedy, W.R., Wendelschafer-Crabb, G., 1993. The innervation of human epidermis. *J. Neurol. Sci.* 115, 184–190.
- Kong, J., White, N.S., Kwong, K.K., Vangel, M.G., Rosman, I.S., Gracely, R.H., Gollub, R.L., 2006. Using fMRI to dissociate sensory encoding from cognitive evaluation of heat pain intensity. *Hum. Brain Mapp.* 27, 715–721.
- Lauria, G., Hsieh, S.T., Johansson, O., Kennedy, W.R., Leger, J.M., Mellgren, S.I., Nolano, M., Merkies, I.S., Polydefkis, M., Smith, A.G., Sommer, C., Valls-Sole, J., European Federation of Neurological Societies/Peripheral Nerve Society Guideline on the use of skin biopsy in the diagnosis of small fiber neuropathy. Report of a joint task force of the European Federation of Neurological Societies and the Peripheral Nerve Society. *Eur. J. Neurol.* 17, 903–912 (e944-909).
- Mazzola, L., Isnard, J., Mauguere, F., 2006. Somatosensory and pain responses to stimulation of the second somatosensory area (SII) in humans. A comparison with SI and insular responses. *Cereb. Cortex* 16, 960–968.
- McArthur, J.C., Stocks, E.A., Hauer, P., Cornblath, D.R., Griffin, J.W., 1998. Epidermal nerve fiber density: normative reference range and diagnostic efficiency. *Arch. Neurol.* 55, 1513–1520.
- McLaren, D.G., Ries, M.L., Xu, G., Johnson, S.C., 2012. A generalized form of context-dependent psychophysiological interactions (gPPI): a comparison to standard approaches. *Neuroimage* 61, 1277–1286.
- Merksey, H., Bogduk, N., 1994. Classification of Chronic Pain. IASP Press, Seattle.
- Ochsner, K.N., Ludlow, D.H., Knierim, K., Hanelin, J., Ramachandran, T., Glover, G.C., Mackey, S.C., 2006. Neural correlates of individual differences in pain-related fear and anxiety. *Pain* 120, 69–77.
- Ostrowsky, K., Magnin, M., Rylvlin, P., Isnard, J., Guenot, M., Mauguere, F., 2002. Representation of pain and somatic sensation in the human insula: a study of responses to direct electrical cortical stimulation. *Cereb. Cortex* 12, 376–385.
- Pan, C.L., Lin, Y.H., Lin, W.M., Tai, T.Y., Hsieh, S.T., 2001. Degeneration of nociceptive nerve terminals in human peripheral neuropathy. *Neuroreport* 12, 787–792.
- Peltz, E., Seifert, F., DeCol, R., Dorfler, A., Schwab, S., Maihofner, C., 2011. Functional connectivity of the human insular cortex during noxious and innocuous thermal stimulation. *Neuroimage* 54, 1324–1335.
- Peyron, R., Laurent, B., Garcia-Larrea, L., 2000. Functional imaging of brain responses to pain. A review and meta-analysis (2000). *Neurophysiol. Clin.* 30, 263–288.
- Ringkamp, M., Raja, S.N., Campbell, J.N., Meyer, R.A., 2013. Peripheral Mechanisms of Cutaneous Nociception. 6th ed. Elsevier Churchill Livingstone, Philadelphia.
- Robinson, C.J., Burton, H., 1980. Somatic submodality distribution within the second somatosensory (SII), 7b, retroinsular, postauditory, and granular insular cortical areas of M. fascicularis. *J. Comp. Neurol.* 192, 93–108.
- Schmahmann, J.D., Leifer, D., 1992. Parietal pseudothalamic pain syndrome. Clinical features and anatomic correlates. *Arch. Neurol.* 49, 1032–1037.
- Selim, M.M., Wendelschafer-Crabb, G., Hodges, J.S., Simone, D.A., Foster, S.X., Vanhove, G.F., Kennedy, W.R., 2010. Variation in quantitative sensory testing and epidermal nerve fiber density in repeated measurements. *Pain* 151, 575–581.
- Timmermann, L., Ploner, M., Hauke, K., Schmitz, F., Baltissen, R., Schnitzler, A., 2001. Differential coding of pain intensity in the human primary and secondary somatosensory cortex. *J. Neurophysiol.* 86, 1499–1503.
- Todd, A.J., Koerber, H.R., 2013. Neuroanatomical Substrates of Spinal Nociception. 6th ed. Elsevier Churchill Livingstone, Philadelphia.
- Treede, R.D., Kenshalo, D.R., Gracely, R.H., Jones, A.K., 1999. The cortical representation of pain. *Pain* 79, 105–111.
- Tseng, M.T., Hsieh, S.C., Shun, C.T., Lee, K.L., Pan, C.L., Lin, W.M., Lin, Y.H., Yu, C.L., Hsieh, S.T., 2006. Skin denervation and cutaneous vasculitis in systemic lupus erythematosus. *Brain* 129, 977–985.

- Tseng, M.T., Tseng, W.Y.I., Chao, C.C., Lin, H.E., Hsieh, S.T., 2010. Distinct and shared cerebral activations in processing innocuous versus noxious contact heat revealed by functional magnetic resonance imaging. *Hum. Brain Mapp.* 31, 743–757.
- Tseng, M.T., Chiang, M.C., Chao, C.C., Tseng, W.Y., Hsieh, S.T., 2013a. fMRI evidence of degeneration-induced neuropathic pain in diabetes: enhanced limbic and striatal activations. *Hum. Brain Mapp.* 34, 2733–2746.
- Tseng, M.T., Chiang, M.C., Yazhuo, K., Chao, C.C., Tseng, W.Y., Hsieh, S.T., 2013b. Effect of aging on the cerebral processing of thermal pain in the human brain. *Pain* 154, 2120–2129.
- Turk, D.C., Melzack, R., 1992. *The measurement and assessment of people in pain*. The Guildford Press, New York.
- Tzourio-Mazoyer, N., Landeau, B., Papathanassiou, D., Crivello, F., Etard, O., Delcroix, N., Mazoyer, B., Joliot, M., 2002. Automated anatomical labeling of activations in SPM using a macroscopic anatomical parcellation of the MNI MRI single-subject brain. *Neuroimage* 15, 273–289.
- Wiech, K., Lin, C.S., Brodersen, K.H., Bingel, U., Ploner, M., Tracey, I., 2010. Anterior insula integrates information about salience into perceptual decisions about pain. *J. Neurosci.* 30, 16324–16331.
- Wiech, K., Jbabdi, S., Lin, C.S., Andersson, J., Tracey, I., 2014. Differential structural and resting state connectivity between insular subdivisions and other pain-related brain regions. *Pain* 155, 2047–2055.
- Willis Jr., W.D., Zhang, X., Honda, C.N., Giesler Jr., G.J., 2001. Projections from the marginal zone and deep dorsal horn to the ventrobasal nuclei of the primate thalamus. *Pain* 92, 267–276.
- Zhou, L., Kitch, D.W., Evans, S.R., Hauer, P., Raman, S., Ebenezer, G.J., Gerschenson, M., Marra, C.M., Valcour, V., Diaz-Arrastia, R., Goodkin, K., Millar, L., Shriver, S., Asmuth, D.M., Clifford, D.B., Simpson, D.M., McArthur, J.C., Narc, Group, A.A.S., 2007. Correlates of epidermal nerve fiber densities in HIV-associated distal sensory polyneuropathy. *Neurology* 68, 2113–2119.